The performance of different density functional methods in the calculation of molecular structures and vibrational spectra of platinum(II) antitumor drugs: Cisplatin and carboplati...

ARTICLE *in* JOURNAL OF COMPUTATIONAL CHEMISTRY · JULY 2001

Impact Factor: 3.59 · DOI: 10.1002/jcc.1053 · Source: DBLP

2 AUTHORS:

Rafał Wysokiński
Wroclaw University of Technology
19 PUBLICATIONS **591** CITATIONS
SEE PROFILE

Danuta Michalska
Wroclaw University of Technology
97 PUBLICATIONS **2,247** CITATIONS
SEE PROFILE

The Performance of Different Density Functional Methods in the Calculation of Molecular Structures and Vibrational Spectra of Platinum(II) Antitumor Drugs: Cisplatin and Carboplatin

RAFAŁ WYSOKIŃSKI, DANUTA MICHALSKA

Institute of Inorganic Chemistry, I-5, Wrocław University of Technology, Smoluchowskiego 23, 50–370 Wrocław, Poland

Received 22 May 2000; accepted 11 January 2001

ABSTRACT: A comparison of eight density functional models for predicting the molecular structures, vibrational frequencies, infrared intensities, and Raman scattering activities of platinum(II) antitumor drugs, cisplatin and carboplatin, is reported. Methods examined include the pure density functional protocols (G96LYP, G96PW91, modified mPWPW and original PW91PW91), one-parameter hybrid approaches (mPW1PW and mPW1LYP), and three-parameter hybrid models (B3LYP and B3PW91), as well as the HF and MP2 levels of theory. Different effective core potentials (ECPs) and several basis sets are considered. The theoretical results are discussed and compared with the experimental data. It is remarkable that the mPW1PW protocol introduced by Adamo and Barone [J Chem Phys 1998, 108, 664], is clearly superior to all the remaining density functional methods (including B3LYP). The geometry and vibrational frequencies of cisplatin and carboplatin calculated with the mPW1PW method, and the ECP of Hay and Wadt (LanL2DZ basis set) are in better agreement with experiment than those obtained with the MP2 method. The use of more elaborated ECP and the enlargements of basis sets do not significantly improve the results. A clear-cut assignments of the platinum-ligand vibrations in cisplatin and carboplatin are presented. It is concluded that mPW1PW is the new reliable method, which can be used in predicting molecular structures and vibrational spectra of large coordination compounds containing platinum(II). © 2001 John Wiley & Sons, Inc. J Comput Chem 22: 901–912, 2001

Correspondence to: D. Michalska; e-mail: michalska@ichn.ch.pwr.wroc.pl

Journal of Computational Chemistry, Vol. 22, No. 9, 901–912 (2001)

Keywords: density functional theory; vibrational frequencies; infrared intensities; Raman activities; cisplatin; carboplatin; platinum(II) complexes; antitumor

Introduction

The long-standing interest in platinum(II) complexes stems from the well-established anticancer activity of these compounds. The discovery of *cis*-diamminedichloroplatinum(II), *cis*-[$PtCl_2(NH_3)_2$] as an antitumor drug (clinically known as cisplatin)[1] has led to the numerous experimental[2–5] and theoretical[6–9] investigations on the molecular properties and the mechanism of action of this compound. Today, cisplatin is frequently used in clinical therapy, and is considered as a very successful drug, mainly against testicular carcinomas but also against ovarian carcinomas, and tumors of the head and neck.[6] Although the nephrotoxicity of cisplatin can be repressed, other toxic side effects have been severe, and in fact, stimulated intensive research towards the design of new platinum chemotherapeutic agents.[10–12] The second generation platinum drug, carboplatin, [*cis*-diammine-(1,1-cyclobutanedicarboxylato)platinum(II)], has received worldwide approval in a routine clinical use.[13] The structures of cisplatin and carboplatin are illustrated in Scheme 1.

In continued search of new platinum drugs of the improved anticancer activity, over 3000 cisplatin analogues[14] and other platinum(II) and platinum(IV) complexes have been prepared and tested against various types of tumors.[6, 10–12] Accurate theoretical prediction of molecular structures using advanced quantum-chemical methods can greatly facilitate the design of a new compound. Moreover, reliable prediction of both the vibrational frequency and IR intensity (or Raman activity) of the vibration, makes it possible to identify the novel molecule, because agreement between the theoretical and experimental infrared and Raman spectra indicates that the calculated molecular geometry is correct. We have shown earlier[15] that in the case when the molecular structure of a new compound cannot be established directly by means of X-ray analysis, the *ab initio* predicted frequencies and infrared intensities complemented with the experimental studies of vibrational spectra play a major role in elucidating the structure of the compound.

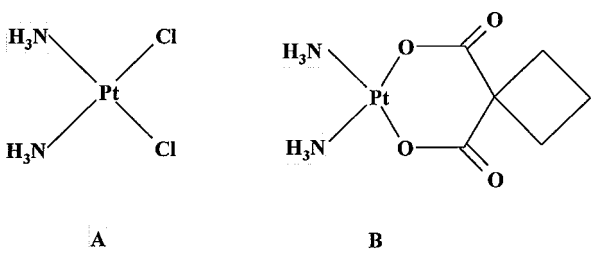

SCHEME 1. The structures of:
(A) *cis*-diamminedichloroplatinum(II), cisplatin; and
(B) *cis*-diammine-(1,1-cyclobutanedicarboxylato)-platinum(II), carboplatin.

During the past several years, the density functional theory (DFT) has emerged as a promising alternative to conventional *ab initio* HF and MP2 methods in computational chemistry. In particular, the implementation of analytic second derivatives of the gradient-corrected density functional energy[16] and the recent progress in the nonlocal (gradient-corrected) functionals,[17–22] have raised the accuracy of calculations of the molecular structures and vibrational spectra. Recently, several research groups[23–26] have demonstrated that the gradient-corrected methods are efficient and accurate computational tools in the studies of real reaction systems containing transition metals. Dedieu[27] reported a comprehensive overview on theoretical studies in Pt and Pd chemistry. The bonding and structures of trans-$Pt(NH_3)_2^{2+}$ complexes with DNA nucleobases have been investigated with a DFT approach by Carloni and Andreoni[28] and by other workers[29] (using B3LYP method). Despite large interest in theoretical platinum chemistry, there are only a few reports on the application of DFT methods to study of the vibrational spectra of platinum complexes. Jonas and Thiel[30] performed calculations of the vibrational spectra of the series of transition metal carbonyls (including Pt) by using nonhybrid gradient corrected functionals (BP86, BLYP, and PW91) and compared the theoretical results with the experimental infrared spectra. Unfortunately, only three vibrations (two C—O stretchings and one Pt—C stretching) have been observed for $Pt(CO)_4$ in the Ar matrix at low temperatures (this compound is very unstable at room temperature).[30] Pavankumar et al.[8] performed quantum chemical calculations on the structure and vibrations of cisplatin using the HF and post-HF methods and various basis sets, and they have

concluded that the MP2/6–311G* and HF/6–311G* levels of theory are the best choice for studying molecular properties of Pt complexes. It is known, however, that the HF method is often insufficient for reliable predictions of vibrational frequencies and infrared intensities, whereas the DFT-based methods, which include a significant fraction of electron correlation, give results of a quality comparable to (or even better than) that obtained with the second-order Möller–Plesset perturbation theory.[16, 31]

So far, no attempt has been made to analyze the application of various DFT methods and different effective core potentials (ECPs) for accurate calculations of vibrational spectra of large platinum(II) complexes. The first purpose of this work is to investigate the performance of different DFT methods in predicting geometry, vibrational frequencies, infrared intensities, and Raman scattering activities of two platinum(II) complexes: cisplatin and carboplatin. In particular, the two novel DFT models, mPWPW and mPW1PW, introduced recently by Adamo and Barone,[17] seem to be very promising, because they have yielded remarkable results for covalent and noncovalent interactions in several compounds.

The second purpose of this study is to provide reliable assignment of the platinum–ligand vibrations in cisplatin and carboplatin. This can be used in further spectroscopic investigations of biological systems containing platinum(II).

Methods

All the DFT computations performed in this work are based on the Kohn–Sham (KS)[32] approach to the density functional theory (as implemented in the recent version of the Gaussian package[33]). We have considered different density functional methods: pure DFT, three-parameter hybrid, and one-parameter hybrid protocols. Among the pure DFT functionals, the following four were applied: (a) mPWPW, introduced by Adamo and Barone[17] (the modification of the gradient-corrected Perdew–Wang exchange functional, PW91, combined with the nonlocal correlation functional); (b) original PW91PW91,[18] abbreviated as PWPW; (c) combination of the gradient-corrected exchange functional proposed by Gill (G96)[19] and PW91 correlation functional (referred to as G96PW); and (d) combination of the G96 exchange and the LYP (Lee–Yang–Parr) correlation functional[20] (abbreviated as G96LYP). It should be noted that G96 is the simplest exchange functional of all approaches considered.[19] Of the three-parameter hybrid protocols we have used the well-known B3LYP[20, 21] and B3PW91[18] methods (the latter abbreviated as B3PW). We have also applied the following one-parameter hybrid models: mPW1PW, introduced by Adamo and Barone,[17] which is the Becke-style one-parameter functional coupled with the modified Perdew–Wang exchange and correlation functionals; and mPW1LYP, where the nonlocal correlation is provided by the LYP expression. It should be mentioned that both the mPW1PW and mPW1LYP protocols are true adiabatic connection models, i.e., they do not contain optimized parameters for the mixing of exact and density functional exchange. For comparison, calculations were also performed with Hartree–Fock and the second-order Möller–Plesset (MP2) methods.[34]

We have used three different effective core potentials (ECPs), which substitute the innermost core orbitals of platinum atom and simultaneously account for the relativistic effects, being important in *ab initio* calculations on heavy atoms. The ECP by Hay and Wadt[35, 36] and the concomitant basis set (LanL2DZ), employs the (8s6p3d)/[5s3p2d]-GTO valence basis set for platinum atom. The valence electron shell for platinum includes both $n = 5$(s,p,d) and $n = 6$(s) orbitals. Calculations were also performed with the LanL2DZ basis set augmented by 5D-polarization functions on heavy atoms, using the following exponents: 0.864 for N; 0.514 for Cl; and 0.0747 for Pt.[36] The second ECP applied was the Stuttgart/Dresden potential with the corresponding SDD basis set.[37] This method employs the (8s7p6d)/[6s5p3d] –GTO valence basis set for Pt. The third ECP, compact effective pseudopotential of Stevens, Basch and Krauss,[38] has been used with the triple-split valence basis set (CEP-121G). This choice leads to the (7sp5d)/[4sp3d]-GTO valence basis set for Pt.

Five possible configurations of *cis*- $[PtCl_2(NH_3)_2]$ (which differed in the positions of the hydrogen atoms) were optimized under the symmetry constraints imposed by the point groups: two of C_{2v}, two of C_s, and one of C_2 symmetry. For carboplatin no symmetry constraints were imposed on the structure. At each theory level, the geometry optimization was followed by calculations of harmonic frequencies, infrared intensities, and Raman activities. The frequencies of NH_3 stretching and bending vibrations calculated with the use of MP2 and the DFT hybrid methods (B3LYP, B3PW, mPW1PW, mPW1LYP) were scaled by a uniform scaling factor of 0.945, whereas those calculated with the HF method were scaled by 0.88. The values of this scaling factor were obtained by a least-squares fit of the

calculated to the observed frequencies, similarly to our previous study on molecules containing the NH groups.[39] It should be emphasized that the frequencies of vibrations involving a motion of the platinum atom in cisplatin and carboplatin were not scaled. For pure DFT protocols (mPWPW, PWPW, G96PW, G96LYP) no uniform scaling factor could be applied; therefore, all the calculated frequencies were left unscaled. To provide the unequivocal vibrational assignment, the potential energy distributions (PEDs) have been calculated at each theory level, according to the procedure described earlier.[31, 39, 40] This allowed us to obtain a detailed insight into the nature of all normal modes of cisplatin and carboplatin.

Calculations have been carried out with the Gaussian 98 package[33] running on Cray J916 and the CSGI Origin 2000 supercomputers.

Results and Discussion

GEOMETRY OF CISPLATIN

According to the results obtained with all theoretical methods, the lowest energy structure of cisplatin is of C_{2v} symmetry. In this configuration, the two hydrogen atoms from two ammonia groups are lying in the molecular plane in the N—Pt—Cl quadrants. The calculated geometrical parameters are listed in Table I. For comparison, the experimental results from X-ray crystal analysis of cisplatin[41] are shown under the table. It should be noted that the intermolecular interactions in solid cisplatin lead to significant distortion of the $PtCl_2N_2$ skeleton (the two Pt—N bonds are reported to be unequal by about 0.1 Å).[41] Therefore, the experimental results for solid cisplatin cannot serve as a rigorous check for the theoretical studies. However, the calculated values may also be compared to the observed Pt—N distances in $Pt(NH_3)_4^{2+}$ (2.05 Å)[42] and Pt—Cl distances in $PtCl_4^{2-}$ (2.32 Å),[43] where interactions in crystal are much weaker. In Table I, in columns 1–11, we have compared the results obtained from the *ab initio* and DFT calculations using LanL2DZ basis set. It is seen that the Pt—N bond distances yielded by the HF, MP2, and G96LYP methods are significantly overestimated, whereas that calculated with the mPW1PW protocol (2.085 Å) is nearest the experimental data. Furthermore, mPW1PW predicts the Pt—Cl bond length (2.386 Å) in better agreement with experiment than all other methods.

TABLE I.
Comparison of Bond Lengths (in Å) and Bond Angles (in deg) Calculated for Cisplatin with HF, MP2, and Various DFT Methods.

						LanL2DZ					mPW1PW			
Geometry	HF	MP2	mPWPW	PWPW	G96PW	G96LYP	B3LYP	B3PW	mPW1LYP	mPW1PW	LanL2DZ[a]	LanL2DZ[b]	SDD[c]	CEP-121G[d]
r(Pt—N)	2.126	2.123	2.099	2.096	2.095	2.121	2.110	2.091	2.110	2.085	2.078	2.086	2.084	2.090
r(Pt—Cl)	2.415	2.406	2.408	2.405	2.404	2.430	2.411	2.393	2.409	2.386	2.385	2.320	2.368	2.361
∠(N—Pt—N)	95.7	97.5	100.3	100.4	100.2	100.2	99.2	99.3	99.1	99.2	98.9	98.6	98.7	98.1
∠(Cl—Pt—Cl)	97.1	96.0	96.7	96.7	96.7	97.0	96.8	96.4	96.7	96.3	95.9	95.5	95.9	95.4

[a] LanL2DZ basis set augmented by 5D-polarization functions on nitrogen atoms.
[b] LanL2DZ augmented by 5D-polarization functions on all heavy atoms (N, Cl, Pt). See text for the exponents.
[c] Stuttgart/Dresden ECP.
[d] SBK (Stevens, Basch, Krauss) effective core potential. Experimental X-ray crystal data for cisplatin are: Pt—N = 2.01 ± 0.04, Pt—Cl = 2.33 ± 0.01, N—Pt—N = 87 ± 1.5, Cl—Pt—Cl = 91.9 ± 0.4; ref. 41.

The G96LYP and HF methods yield significantly too long Pt—Cl distances (2.430 and 2.415 Å, respectively). It seems that the G96LYP protocol is the most deficient in predicting molecular geometry for cisplatin. However, it is interesting to note that the G96PW model (G96 exchange functional combined with the Perdew–Wang correlation functional) yields better results than G96LYP. The remaining pure density functionals, mPWPW and PWPW, overestimate the Pt—N and Pt—Cl bond lengths by about 0.01 and 0.02 Å, respectively, compared to the mPW1PW results. Also the remaining hybrid models (mPW1LYP, B3LYP, and B3PW) yield too long bond distances for platinum–ligands. It follows from this comparison that the mPW1PW hybrid model is clearly superior to all other theoretical methods in predicting the Pt—N and Pt—Cl bond lengths in cisplatin.

The calculated N—Pt—N angle varies in the range from 95.7° (HF) to 100.3° (mPWPW), whereas the experimental value is equal to 87°. Moreover, the calculated Cl—Pt—Cl angle is also larger than experimental, by about 4–5°. Similar values of the bond angles in cisplatin have also been obtained in the theoretical studies with the post-HF methods.[8] These results indicate that in a bare cisplatin (in the gas phase) the intramolecular N—H. . .Cl interaction opens up both the N—Pt—N and Cl—Pt—Cl angles. The calculated at the MP2/SDD level, the H. . .Cl distance of about 2.5 Å and the N—H. . .Cl angle of 112° indicate a weak hydrogen bonding. It seems however, that in solid cisplatin, the intermolecular interaction or steric repulsion between the neighboring molecules becomes more important than the intramolecular hydrogen bonding; therefore, the experimental values of both the N—Pt—N and Cl—Pt—Cl bond angles are smaller than those theoretically predicted for the free molecule.

We have investigated the effects of the basis sets on the calculated geometry of cisplatin by the use of the mPW1PW method and various effective core potentials and basis sets. The results are shown in columns 12–15 of Table I. Calculations performed with the LanL2DZ basis set augmented by 5D-polarization functions on the nitrogen atoms yielded little improvement in the predicted Pt—N bond length. When the 5D sets of polarization functions were added to all heavy atoms (N, Cl, Pt), the calculated Pt—N bond distance was almost unaffected, whereas the computed Pt—Cl bond length (2.320 Å) showed excellent agreement with the experimental value (2.33 ± 0.01 Å). The Stuttgart/Dresden ECP and SDD basis set[37] yielded the bond lengths and angles (column 14) similar to those obtained with LanL2DZ. The compact potential of Stevens, Basch, and Krauss[38] and the CEP-121G basis set yielded the Pt—N distance slightly too long, compared to both the SDD and LanL2DZ results.

VIBRATIONAL SPECTRA OF CISPLATIN

Despite the numerous studies on the vibrational spectra of cisplatin,[44–49] the assignment of some bands is still controversial. For example, Pavankumar et al.[8] attributed the calculated frequency of the N—Pt—N bending vibration to the experimental band at 222 cm^{-1}, following the earlier paper by Nakamoto et al.[44] However, the others[45] assigned this vibration at 250 cm^{-1} in the infrared spectrum of cisplatin. Therefore, in this work, we have measured new FTIR and FT-Raman spectra of *cis*-$[PtCl_2(NH_3)_2]$ and compared it with the theoretical results. In Table II are shown the characteristic bands observed in the IR and Raman spectra of cisplatin, and the theoretical harmonic frequencies, infrared intensities, and Raman activities of vibrations, computed with the MP2 and mPW1PW methods, using several basis sets. A clearcut assignment of the bands has been obtained from the calculated potential energy distribution (the symmetry coordinates, and the detailed vibrational assignment for cisplatin, and carboplatin will be published elsewhere[50]). Table III compares the results obtained with HF, MP2, and different DFT methods for cisplatin. Figure 1 illustrates the theoretical infrared spectra in the low-frequency region (600–50 cm^{-1}), calculated with several methods, and the experimental data from our studies. Although it may be expected that the low-frequency modes are very anharmonic, quite a good overall agreement between the theoretical and experimental spectra has been obtained.

Platinum–Nitrogen and Platinum–Chlorine Vibrations

As is seen in Figure 1, the spectra predicted with the MP2, mPW1PW, and B3LYP methods are very similar. The HF method overestimates the infrared intensities of Pt—Cl stretching vibrations (the corresponding experimental bands are observed at 318/326 cm^{-1}). Another feature of interest is that the theoretical infrared intensities of the Pt—N stretching vibrations are consistently larger than the experimental bands, observed at 510 and 517 cm^{-1}. It is worth mentioning that the calculated results refer to the molecule in the gas phase at 0 K, whereas comparison is made with the infrared spectra of solid

TABLE II.

Theoretical Harmonic Frequencies[a] (cm^{-1}), Infrared Intensities[b] (km/mol), and Raman Activities[c] ($Å^4$/amu) Calculated for Cisplatin with MP2 and Density Functional (mPW1PW) Methods Using Various Basis Sets: Experimental Frequencies Are for Solid. Vibrational Assignment Is Based on the Calculated Potential Energy Distribution (PED).

Mode No.	Sym	Exp.[d] IR	Exp.[d] R	MP2 SDD	MP2 LanL2DZ	mPW1PW SDD	mPW1PW LanL2DZ	mPW1PW LanL2DZ[e]	mPW1PW LanL2DZ[f]	Assignment PED (%)
Q7	A_1	253 s	253 s	232 [25, 3]	226 [26, 4]	236 [25, 2]	236 [26, 3]	233 [26, 3]	230 [27, 3]	β(N—Pt—N) (95)
Q8	B_2	318 vs		348 [31, 9]	340 [29, 11]	339 [30, 7]	334 [26, 9]	335 [26, 9]	335 [26, 6]	asym ν(Pt—Cl)(100)
Q9	A_1	326 sh	322 vs	354 [24, 13]	347 [24, 14]	349 [26, 9]	344 [25, 10]	344 [24, 10]	349 [24, 7]	sym ν(Pt—Cl)(98)
Q10	B_2	510 w	506 s	489 [13, 9]	466 [16, 9]	490 [12, 5]	490 [13, 5]	479 [12, 5]	467 [8, 5]	asym ν(Pt—N)(98)
Q11	A_1	517 sh	522 vs	493 [4, 14]	470 [5, 17]	496 [2, 10]	495 [2, 11]	485 [2, 12]	474 [1, 10]	sym ν(Pt—N)(100)
Q15	A_1	795 s	809 w	817 [76, 12]	808 [78, 12]	817 [89, 11]	827 [88, 10]	793 [77, 7]	782 [87, 6]	$\rho_r(NH_3)$(96)
Q16	B_2	1298 vs	1294 w	1280 [242, 4]	1274 [294, 15]	1245 [274, 0]	1250 [313, 5]	1249 [195, 6]	1239 [195, 2]	$\delta_s(NH_3)$(100)
Q17	A_1	1312 vs	1314 w	1287 [164, 2]	1282 [193, 10]	1251 [185, 2]	1256 [196, 3]	1255 [111, 4]	1246 [119, 3]	$\delta_s(NH_3)$(100)
Q20	A_2		1625 w	1634 [0, 12]	1640 [0, 11]	1632 [0, 13]	1627 [0, 12]	1614 [0, 10]	1616 [0, 10]	$\delta_d(NH_3)$(100)
Q21	B_1	1626 m		1641 [64, 1]	1645 [73, 1]	1638 [66, 1]	1633 [74, 1]	1621 [60, 1]	1624 [50, 0]	$\delta_d(NH_3)$(100)
Q23	A_1	3203 s	3210 s	3190 [21, 193]	3195 [21, 165]	3206 [87, 205]	3200 [94, 193]	3228 [53, 184]	3230 [58, 182]	$\nu(NH_3)$(90)
Q25	A_1	3285 vs	3306 m	3332 [71, 65]	3343 [83, 64]	3377 [72, 110]	3377 [80, 107]	3370 [92, 105]	3372 [88, 107]	$\nu(NH_3)$(90)
τCPU[g]				910	136	219	111	245	368	

[a] Frequencies of the modes: Q_{15} to Q_{25} scaled by 0.945, see text.
[b] IR intensity: the first value in square brackets.
[c] Raman activity: the second value in square brackets.
[d] Experimental infrared (IR) and Raman (R) data for solid, our data.
[e] LanL2DZ augmented with polarization functions on N atoms.
[f] LanL2DZ augmented with polarization functions on N, Cl, Pt atoms.
[g] CPU time (min) of calculating frequencies, IR intensities and Raman activities.
Abbreviations: br, broad; m, medium; s, strong; sh, shoulder; v, very; w, weak; asym, antisymmetric; sym, symmetric; ν, stretching; β, in-plane bending; δ_d, NH_3 degenerate deformation; δ_s, NH_3 symmetric deformation; ρ_r, NH_3 rocking.

molecule, taken at room temperature. This may partially account for the observed differences in the infrared intensities of ν(Pt—N) modes. From the results presented in Table III it is clear that frequencies of the Pt—N stretching vibrations (modes Q_{10} and Q_{11}) predicted with the mPW1PW method (the last column) are the most accurate. It should be emphasized that further enlargements of the LanL2DZ basis set do not introduce important improvements in the calculated infrared intensities or Raman activities of these modes; however, they increase the CPU time, as shown in the bottom line of Table II. As follows from the results presented in Table III, the frequencies of the Pt—N stretching vibrations calculated with the HF and G96LYP methods show the largest deviation from experiment. In Table IV are gathered the theoretical predictions of platinum–ligand vibrations obtained by the use of HF method and various basis sets. For the symmetric Pt—N stretching vibration, sym ν(Pt—N), which is observed as the very strong band at 522 cm^{-1} in the Raman spectrum (and a very weak shoulder at 517 cm^{-1} in IR) the HF-calculated frequencies are: 455 cm^{-1} (CEP-121G); 463 cm^{-1} (SDD); 462 cm^{-1}

TABLE III.

Comparison of the Harmonic Frequencies[a] (cm^{-1}), Infrared Intensities[b] (km/mol), and Raman Activities[c] ($Å^4$/amu) Calculated with HF, MP2, and Various Density Functional Methods, Using LanL2DZ Basis Set: Experimental Frequencies Are for Solid Cisplatin.

Mode No.	Sym	Exp.[d] IR	Exp.[d] R	HF	MP2	mPWPW	PWPW	G96PW	G96LYP	B3LYP	B3PW	mPW1LYP	mPW1PW
Q7	A_1	253 s	253 s	235 [20, 1]	226 [26, 4]	228 [25, 4]	229 [25, 4]	230 [27, 4]	219 [24, 4]	225 [25, 4]	233 [26, 3]	225 [24, 4]	236 [26, 3]
Q8	B_2	318 vs		325 [39, 4]	340 [29, 11]	320 [22, 11]	322 [21, 11]	321 [22, 11]	308 [21, 13]	321 [25, 11]	330 [25, 10]	323 [26, 10]	334 [26, 9]
Q9	A_1	326 sh	322 vs	334 [36, 4]	347 [24, 14]	330 [23, 11]	332 [23, 11]	331 [24, 11]	318 [23, 12]	330 [25, 11]	339 [25, 10]	332 [25, 11]	344 [25, 10]
Q10	B_2	510 w	506 s	451 [15, 4]	466 [16, 9]	472 [10, 5]	477 [10, 5]	474 [11, 5]	448 [12, 5]	463 [14, 5]	483 [13, 5]	465 [14, 5]	490 [13, 5]
Q11	A_1	517 sh	522 vs	462 [6, 7]	470 [5, 17]	476 [1, 12]	481 [1, 12]	476 [1, 12]	452 [1, 12]	468 [2, 12]	487 [2, 12]	470 [3, 12]	495 [2, 11]
Q15	A_1	795 s	809 w	802 [101, 9]	808 [78, 12]	845 [79, 11]	848 [77, 10]	847 [89, 12]	834 [78, 11]	811 [81, 10]	819 [87, 11]	816 [80, 10]	827 [88, 10]
Q16	B_2	1298 vs	1294 w	1284 [391, 7]	1274 [294, 15]	1252 [256, 2]	1253 [256, 2]	1256 [264, 2]	1244 [253, 2]	1229 [298, 5]	1236 [304, 5]	1240 [304, 5]	1250 [313, 5]
Q17	A_1	1312 vs	1314 w	1294 [278, 7]	1282 [193, 10]	1256 [156, 3]	1256 [159, 3]	1260 [159, 3]	1247 [151, 3]	1234 [183, 3]	1242 [189, 3]	1246 [190, 3]	1256 [196, 3]
Q20	A_2		1625 w	1633 [0, 11]	1640 [0, 11]	1661 [0, 15]	1658 [0, 15]	1666 [0, 15]	1661 [0, 16]	1613 [0, 14]	1617 [0, 13]	1623 [0, 13]	1627 [0, 12]
Q21	B_1	1626 m		1639 [100, 0]	1645 [73, 1]	1666 [62, 2]	1663 [62, 2]	1672 [61, 2]	1666 [60, 2]	1619 [71, 1]	1623 [72, 1]	1628 [73, 1]	1633 [74, 1]
Q23	A_1	3203 s	3210 s	3209 [16, 140]	3195 [21, 165]	3225 [151, 235]	3219 [153, 226]	3233 [163, 246]	3221 [140, 252]	3166 [86, 205]	3172 [101, 203]	3187 [76, 193]	3200 [94, 193]
Q25	A_1	3285 vs	3306 m	3333 [109, 63]	3343 [83, 64]	3441 [49, 159]	3440 [50, 163]	3453 [48, 157]	3420 [46, 156]	3332 [72, 110]	3353 [74, 113]	3350 [77, 104]	3377 [80, 107]

[a] Frequencies of the modes: Q_{15} to Q_{25} are scaled by 0.88 for HF; and by 0.945 for MP2, B3LYP, B3PW, mPW1LYP, and mPW1PW methods (see text).
[b] IR intensity: the first value in square brackets.
[c] Raman activity: the second value in square brackets.
[d] Experimental frequencies, this work. Other abbreviations as in Table II.

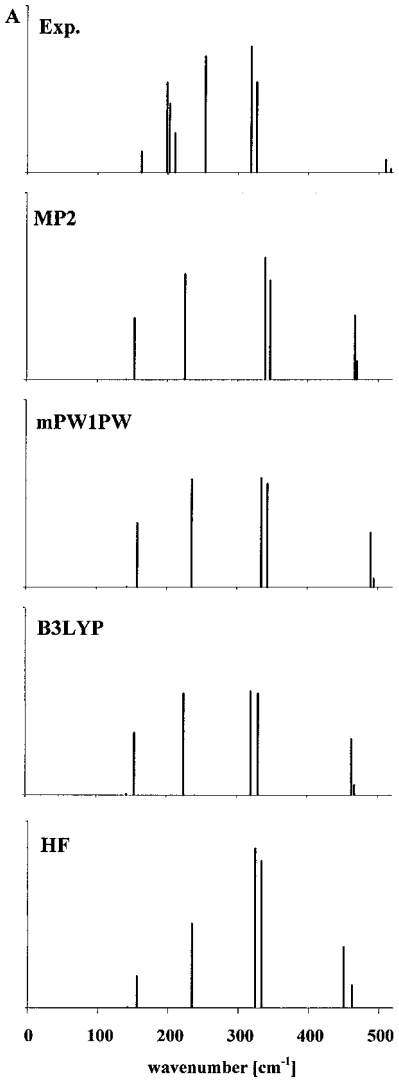

FIGURE 1. Comparison of the theoretical frequencies and infrared intensities calculated with MP2, mPW1PW, B3LYP, and HF methods using LanL2DZ basis set. The experimental frequencies and integral absorption intensities were measured for cisplatin in the solid phase. The remaining lattice modes at 129 and 85 cm^{-1} are not shown.

(LanL2DZ); 451 cm^{-1} (LanL2DZ with 5D polarization functions on N atoms); 449 cm^{-1} (LanL2DZ with 5D set on Cl atoms) and 440 cm^{-1} (LanL2DZ with three 5D sets on N, Cl, and Pt atoms), as shown in Table IV. It is evident that the HF method is inadequate to predicting the Pt—N stretching frequencies regardless of the basis set used.

The frequencies of the Pt—Cl stretching modes (Q_8 and Q_9) calculated with the mPW1PW/LanL2DZ method, show best agreement with experiment, and are almost unaffected by the enlargements of the basis set, as is seen in Table II.

The results gathered in Table III indicate that "pure" density functional methods (mPWPW, PWPW, G96PW, G96LYP) yield quite satisfactory results for the platinum–ligand vibrations (Q_7–Q_{11}). However, the G96LYP functional seems to be inferior to all other theoretical methods. The frequencies of the modes Q_7–Q_{11} are significantly too small, compared to those obtained with the remaining methods. The G96LYP protocol also failed in predicting the bond lengths in cisplatin, as was shown in the previous section. Thus, it seems that this DFT protocol may not be reliable for theoretical studies of platinum(II) complexes. It is interesting, however, that combination of the G96 exchange with PW correlation functional (G96PW protocol) leads to a much better agreement with experimental data.

Vibrations of the NH_3 Groups

The NH_3 vibrations are known to be strongly anharmonic; therefore, the double harmonic approximation (being inherent in the calculations of the force constants and dipole moment derivatives with Gaussian98 program) may not be adequate for describing these strongly anharmonic normal modes. The two strong bands at 3285 and 3203 cm^{-1} in the infrared spectrum of cisplatin have been assigned to the N—H stretching vibrations (modes Q_{25} and Q_{23}, respectively). The frequency of Q_{25} is somewhat overestimated by theory, which can also be attributed to the fact, that intermolecular interactions in solid cisplatin may lower the N—H stretching frequencies. For mode Q_{23}, the frequency is quite well reproduced by calculations with the mPW1PW, MP2, and HF methods; however, the computed infrared intensities show discrepancies between the methods used. In particular, the "pure" functionals significantly overestimate the infrared intensity of this mode, compared with other theoretical results (Table III). The NH_3 degenerate bending modes (δ_d NH_3) have been observed in the range of 1600–1626 cm^{-1} in the infrared and Raman spectra (the origin of the unusual band around 1540 cm^{-1} will be discussed elsewhere[50]). The frequencies, infrared intensities, and Raman scattering activities of the corresponding normal modes, Q_{20} and Q_{21}, are very well predicted by the mPW1PW and other hybrid DFT methods. The NH_3 symmetric bending vibrations, $\delta_s NH_3$, (umbrella-like vibrations[48]) give rise to the strongest bands, at 1298/1312 cm^{-1} in the infrared spectrum of cisplatin. It should be noted that all theoretical methods predicted the highest

TABLE IV.
Comparison of Selected Bond Lenghts (Å), Bond Angles (deg), and Selected Platinum–Ligand Vibrations[abc] for Cisplatin: Calculations with HF Method and Various Basis Sets.

			HF					
	Exp.[d]		CEP-121G	SDD	LanL2DZ	LanL2DZ[e]	LanL2DZ[f]	LanL2D2Z[g]
Geometry								
r(Pt—N)	2.01 ± 0.04		2.131	2.125	2.126	2.119	2.138	2.129
r(Pf—Cl)	2.33 ± 0.01		2.389	2.401	2.415	2.413	2.354	2.352
∠(N—Pt—N)	87 ± 1.5		95.0	95.5	95.7	95.6	95.8	95.5
∠(Cl—Pt—Cl)	91.9 ± 0.4		96.2	96.5	97.1	96.9	96.5	96.2
Vibrations	IR	R						
β(N—Pt—N)	253 s	253 s	232 [18, 2]	236 [19, 1]	235 [20, 1]	232 [20, 2]	231 [22, 1]	230 [21, 1]
asym ν(Pt—Cl)	318 vs		329 [52, 3]	327 [43, 2]	325 [39, 4]	326 [38, 4]	325 [42, 3]	326 [41, 3]
sym ν(Pt—Cl)	326 sh	322 vs	342 [43, 4]	338 [36, 4]	334 [36, 4]	335 [35, 4]	339 [39, 3]	339 [40, 3]
asym ν(Pt—N)	510 w	506 s	441 [12, 3]	451 [14, 3]	451 [15, 4]	439 [14, 3]	438 [12, 3]	427 [10, 3]
sym ν(Pt—N)	517 sh	522 vs	455 [5, 6]	463 [6, 6]	462 [6, 7]	451 [5, 7]	449 [4, 6]	440 [3, 6]

[a] Frequencies (cm^{-1}).
[b] IR intesities (km/mol), the first value in square brackets.
[c] Raman activities ($Å^4$/amu), the second value in square brackets.
[d] Geometrical parameters from ref. 41 and experimental frequencies, our data.
[e] LanL2DZ augmented with polarization functions on N atoms.
[f] LanL2DZ augmented with polarization functions on Cl atoms.
[g] LanL2DZ augmented with polarization functions on N, Cl, Pt atoms. Other abbreviations as in Table II.

infrared intensities for the corresponding modes Q_{16} and Q_{17}, in accordance with experiment. However, the computed frequencies are too low for these modes. Moreover, the calculated infrared intensities and Raman activities show large discrepancies and strong dependence on the basis set used. However, it should be noted that all the theoretical frequencies, infrared intensities, and Raman scattering activities of the characteristic NH_3 rocking vibrations (mode Q_{15}) calculated with the MP2, mPW1PW, mPW1LYP, B3LYP, and B3PW methods are in good agreement with the experiment.

GEOMETRY OF CARBOPLATIN

In carboplatin, the chlorine atoms are replaced with the cyclobutane–dicarboxylate groups, whereas the two ammine groups are in the *cis* position, as shown in Scheme 1B. According to the results obtained with all theoretical methods, the environment of the platinum atom is approximately planar, and the six-membered chelate ring has a boat conformation, which is in agreement with the experimental X-ray diffraction data measured on crystal of carboplatin.[51, 52] Moreover, our calculations have revealed that the cyclobutane ring is slightly puckered, which is also supported by the experimental data. It should be noted that Tornaghi et al.[53] reported planar geometry of the cyclobutane ring in their DFT-optimized structure of carboplatin. In Table V (part A) we have compared the geometrical parameters of the platinum coordination sphere calculated with the mPW1PW, B3LYP, HF, and MP2 methods using the LanL2DZ basis set. The experimental X-ray data for solid cisplatin have also been included.

It follows from this comparison that the Pt—N bond lengths calculated with mPW1PW are nearest the experimental values, whereas those predicted with B3LYP and MP2 methods are slightly too long. The bond angles calculated with the DFT and MP2 methods are similar. Some differences are noted between the theoretical (isolated molecule) and experimental (solid state) bond angles of the platinum

coordination sphere. This can be caused by the intermolecular interaction between the ammonia groups and the carboxylate oxygen atoms of the neighboring molecule in solid carboplatin.[51] It should be noted that all theoretical methods consistently indicate that the Pt—N bond lengths in carboplatin are slightly shorter than those in cisplatin, calculated at the corresponding level of theory.

PLATINUM–LIGAND VIBRATIONS IN CARBOPLATIN

In Table V (part B) we have gathered the frequencies, infrared intensities, and Raman activities of platinum–ligand vibrations are gathered, predicted with various theoretical methods, and the experimental data from the IR and Raman spectra of carboplatin (our data, measured in solid). The assignment of the platinum–ligand vibrations has been made on the basis of the calculated potential energy distribution, PED. As follows from this table, the theoretical frequencies of Pt—N stretching vibrations, calculated with the mPW1PW/LanL2DZ method are nearest the experimental values. The corresponding frequencies, calculated with B3LYP, HF, and MP2 methods, show much larger deviation from experiment. According to the results obtained with the DFT and MP2 methods, the Raman activity of the symmetric (in-phase) Pt—N stretching vibration is high, which is supported by experimental data. However, the HF method yields wrong results for the Raman activity of this vibration (the second value in the square brackets is extremely low).

According to the calculated PED, the Pt—O stretching vibrations are coupled with the chelate ring deformation vibrations and contribute to the bands at 475 and 350 cm^{-1} (infrared). It should be emphasized that the frequencies of these vibrations, predicted at the mPW1PW/LanL2DZ level, 476 and 352 cm^{-1}, respectively, are in perfect agreement with the experiment. Also, the calculated relative infrared intensities and Raman activities

TABLE V.
Comparison of the Selected Bond Lengths (Å), Bond Angles (deg), and Platinum–Ligand Vibrations[a,b,c] for Carboplatin.

			mPW1PW	B3LYP	HF	MP2
	Exp.[d]	Exp.[e]	LanL2DZ			
A Geometry						
r(Pt—N)	2.021	2.010	2.082	2.106	2.121	2.122
r(Pt—O)	2.025	2.029	1.993	2.010	1.989	2.019
∠(O—Pt—N)	87.1	88.2	78.9	78.8	81.4	78.5
∠(O—Pt—O′)	90.5	88.9	96.8	96.6	93.7	97.8
∠(N—Pt—N′)	95.3	93.6	105.4	105.6	103.5	105.0
∠(O—Pt—N′)	177.2	177.9	175.1	175.0	174.9	175.6
B Vibrations[f]	IR	R				
asym ν(Pt—N)	548 vw		501 [2, 2]	471 [2, 12]	470 [3, 2]	475 [3, 13]
sym ν(Pt—N)	540 sh	546 vs	495 [4, 15]	470 [3, 16]	468 [9, 1]	473 [3, 17]
sym ν(Pt—O) + ν(C—C)	475 m	471 s	476 [4, 11]	460 [6, 8]	497 [3, 12]	463 [6, 8]
asym ν(Pt—O) + β(C=O)	350 s	350 w	352 [27, 2]	346 [25, 2]	383 [41, 2]	342 [20, 2]
β(N—Pt—N)	195 m	192 s	205 [45, 2]	199 [39, 2]	196 [42, 1]	199 [43, 2]

[a] Frequencies (cm^{-1}).
[b] IR intesities (km/mol), the first value in square brackets.
[c] Raman activities ($Å^4$/amu), the second value in square brackets.
[d] Geometrical parameters from ref. 51.
[e] From ref. 52.
[f] Experimental frequencies, our data. Other abbreviations as in Table II.

of these vibrations are supported by experimental data. The B3LYP and MP2 methods yielded slightly lower frequencies than experimental, whereas the HF method overestimated them by about 20 and 30 cm^{-1}, respectively. Thus, it is evident that mPW1PW method is superior to all the remaining theoretical methods in predicting molecular structure and vibrational spectra of quite a large platinum(II) complex.

Conclusions

The most important findings of this work are the following:

1. It is remarkable that the mPW1PW protocol (the Becke-style one-parameter functional coupled with the modified Perdew–Wang exchange and correlation functionals)[17] is clearly superior to all the remaining density functional methods (including B3LYP) in predicting the structures, vibrational frequencies, infrared intensities, and Raman scattering activities of cisplatin and carboplatin. Furthermore, calculations performed with the mPW1PW method and the ECP of Hay and Wadt (with the LanL2DZ basis set) yield the geometries and frequencies in better agreement with experiment than those obtained with the MP2 method.
2. The use of more extended basis sets with the mPW1PW functional does not introduce important improvements in the calculated platinum–ligand bond lengths and angles, and vibrational frequencies.
3. The HF method is inadequate to calculation of the Pt—N stretching frequencies (and the corresponding Raman activities of these vibrations) regardless of the basis set used.
4. Pure density functional methods (mPWPW, PWPW, G96PW, and G96LYP) give satisfactory results for vibrational frequencies, however, they do not reproduce well the infrared intensities and Raman activities, especially for the N—H vibrations. G96LYP is the most deficient in predicting molecular geometry and vibrational frequencies for cisplatin.
5. The mPW1PW/LanL2DZ method should be considered among the best performing theory levels in predicting molecular structures and vibrational spectra of large platinum(II) coordination compounds.

Acknowledgments

The Poznań Supercomputer and Networking Center as well as Wrocław Supercomputer and Networking Center are acknowledged for generous allotment of computer time.

References

1. (a) Rosenberg, B.; Van Camp, L.; Krigas, T. Nature 1965, 205, 698; (b) Rosenberg, B.; Van Camp, L.; Trosko, J. E.; Mansour, V. H. Nature 1969, 222, 385.
2. (a) Sherman, S. E.; Lippard, S. J. Chem Rev 1987, 87, 1153; (b) Bruhn, S. L.; Toney, J. H. In Progress in Inorganic Chemistry: Bioinorganic Chemistry; Lippard, S. J., Ed.; Wiley: New York, 1990, p. 477, vol. 38; (c) Bancroft, D. P.; Lepre, C. A.; Lippard, S. J. J Am Chem Soc 1990, 112, 6860.
3. (a) Fichtinger-Schepman, A. M. J.; van der Veer, J. L.; den Hartog, J. H. J.; Lohman, P. H. M.; Reedijk, J. Biochemistry 1985, 24, 707; (b) Reedijk, J.; Fichtinger-Schepman, A. M. J.; Van Osterom, A. T.; Van de Putte, P. Struct Bonding (Berlin) 1987, 67, 53; (c) van der Veer, J. L.; Reedijk, J. Chem Br 1988, 24, 775.
4. (a) Miller, S. E.; House, D. A. Inorg Chim Acta 1991, 187, 125; (b) Miller, S. E.; Gerard, K. J.; House, D. A. Inorg Chim Acta 1991, 190, 135.
5. Jamieson, E. R.; Lippard, S. J. Chem Rev 1999, 99, 2467.
6. (a) Basch, H.; Krauss, M. Stevens, W. J.; Cohen, D. Inorg Chem 1985, 24, 3313; (b) Krauss, M.; Basch, H.; Miller, K. J. Chem Phys Lett 1988, 14, 577.
7. (a) Carloni, P.; Andreoni, W.; Hutter, J.; Curioni, A.; Giannozzi, P.; Parrinello, M. Chem Phys Lett 1995, 234, 50.
8. Pavankumar, P. N. V.; Seetharamulu, P.; Yao, S.; Saxe, J. D.; Reddy, D. G.; Hausheer, F. H. J Comput Chem 1999, 20, 3888.
9. Pelmenschikov, A.; Zilberberg, I.; Leszczynski, J.; Famulari, A.; Sironi, M.; Raimondi, M. Chem Phys Lett 1999, 314, 496.
10. (a) Reedijk, J. Chem Rev 1999, 99, 2499; (b) Reedijk, J. Chem Commun 1996, 801.
11. Lippert, B. Coord Chem Rev 1999, 182, 263.
12. Wong, E.; Giandomenico, C. M. Chem Rev 1999, 99, 2451.
13. Lebwohl, D.; Canetta, R. Eur J Cancer 1998, 34, 1522.
14. Weiss, R. B.; Christian, M. C. Drugs 1993, 46, 360.
15. (a) Michalska, D.; Chojnacki, H.; Hess, B. A., Jr.; Schaad, L. J. Chem Phys Lett 1987, 141, 376; (b) Hess, B. A., Jr.; Michalska, D.; Schaad, L. J. J Am Chem Soc 1985, 107, 1449.
16. Johnson, B. G.; Frisch, M. J. J Chem Phys 1994, 100, 7429.
17. Adamo, C.; Barone, V. J Chem Phys 1998, 108, 664.
18. (a) Burke, K.; Perdew, J. P.; Wang, Y. In Electronic Density Functional Theory: Recent Progress and New Directions; Dobson, J. F.; Vignale, G.; Das, M. P., Eds.; Plenum: New York, 1998; (b) Perdew, J. P.; Burke, K.; Wang, Y. Phys Rev B 1996, 54, 16533; (c) Perdew, J. P.; Wang, Y. Phys Rev B 1992, 45, 13244.
19. Gill, P. M. W. Mol Phys 1996, 89, 433.
20. Lee, C.; Yang, W.; Parr, R. G. Phys Rev B 1988, 37, 785.
21. (a) Becke, A. D. J Chem Phys 1993, 98, 5648; (b) Becke, A. D. J Chem Phys 1996, 104, 1040.

22. Parr, R. G.; Yang, W. Density Functional Theory of Atoms and Molecules; Oxford Univ. Press: Oxford, 1989.
23. Niu, S.; Hall, M. B. Chem Rev 2000, 100, 353.
24. (a) Siegbahn, P. E. M.; Crabtree, R. H. J Am Chem Soc 1999, 121, 117; (b) Siegbahn, P. E. M.; Crabtree, R. H. J Am Chem Soc 1997, 119, 3103; (c) Siegbahn, P. E. M.; Crabtree, R. H. J Am Chem Soc 1996, 118, 4442; (d) Siegbahn, P. E. M. Inorg Chem 1999, 38, 2880; (e) Siegbahn, P. E. M.; Blomberg, M. R. A. Chem Rev 2000, 100, 421.
25. Salahub, D. R.; Castro, M.; Fournier, R.; Calaminici, P.; Godbout, N.; Goursot, A.; Jamorski, C.; Kobayashi, H.; Martinez, A.; Papai, I.; Proynov, E.; Russo, N.; Sirois, S.; Ushio, J.; Vela, A. In Theoretical and Computational Approaches to Interface Phenomena; Sellers, H.; Olab, J., Eds.; Plenum: New York, 1995, p. 187.
26. Musaev, D. G.; Morokuma, K. In Advances in Chemical Physics; Rice, S. A.; Prigogine, I., Eds.; John Wiley & Sons: New York, 1996, p. 61, vol. XCV.
27. Dedieu, A. Chem Rev 2000, 100, 543.
28. Carloni, P.; Andreoni, W. J Phys Chem 1996, 100, 17797.
29. Šponer, J.; Šponer, J. E.; Gorb, L.; Leszczynski, J.; Lippert, B. J Phys Chem A 1999, 103, 11406.
30. Jonas, V.; Thiel, W. J Chem Phys 1995, 102, 8474.
31. (a) Michalska, D.; Bieńko, D. C.; Abkowicz-Bieńko, A. J.; Latajka, Z. J Phys Chem A 1996, 100, 17786; (b) Abkowicz-Bieńko, A. J.; Latajka, Z.; Bieńko, D. C.; Michalska, D. Chem Phys 1999, 250, 123.
32. Kohn, W.; Sham, L. J. Phys Rev 1988, A38, 3098.
33. Frisch, M. J.; Trucks, G. W.; Schlegel, H. B.; Scuseria, G. E.; Robb, M. A.; Cheeseman, J. R.; Zakrzewski, V. G.; Montgomery, J. A.; Stratmann, R. E.; Burant, J. C.; Dapprich, S.; Millam, J. M.; Daniels, A. D.; Kudin, K. N.; Strain, M. C.; Farkas, O.; Tomasi, J.; Barone, V.; Cossi, M.; Cammi, R.; Mennucci, B.; Pomelli, C.; Adamo, C.; Clifford, S.; Ochterski, J.; Petersson, G. A.; Ayala, P. A.; Cui, Q.; Morokuma, K.; Malick, K. D.; Rabuck, A. D.; Raghavachari, K.; Foresman, J. B.; Cioslowski, J.; Ortiz, J. V.; Stefanov, B. B.; Liu, G.; Liashenko, A.; Piskorz, P.; Komaromi, I.; Gomperts, R.; Martin, R. L.; Fox, D. J.; Keith, T.; Al-Laham, M. A.; Peng, C. Y.; Nanayakkara, A.; Gonzales, C.; Challacombe, M.; Gill, P. M. W.; Johson, B. G.; Chen, W.; Wong, M.; Anders, J. L.; Head-Gordon, M.; Replogle, E. S.; Pople, J. A. Gaussian 98 (Revision A1); Gaussian, Inc.: Pittsburgh, PA, 1998.
34. Möller, C.; Plesset, M. S. Phys Rev 1934, 46, 618.
35. (a) Hay, P. J.; Wadt, W. R. J Chem Phys 1985, 82, 270, 299; (b) Wadt, W. R.; Hay, P. J. J Chem Phys 1985, 82, 284.
36. Dunning, T. H., Jr.; Hay, P. J. In Modern Theoretical Chemistry; Schaefer, H. F., III, Ed.; Plenum: New York 1976, 3, 1.
37. Andrae, D.; Haeussermann, U.; Dolg, M.; Stoll, H.; Preuss, H. Theor Chim Acta 1990, 77, 123.
38. (a) Stevens, W. J.; Basch, H.; Krauss, M. J Chem Phys 1984, 81, 6026; (b) Stevens, W. J.; Krauss, M.; Basch, H.; Jasien, P. G. Can J Chem 1992, 70, 612.
39. Bieńko, D. C.; Michalska, D.; Roszak, S.; Wojciechowski, W.; Nowak, M. J.; Lapinski, L. J Phys Chem A 1997, 101, 7834.
40. Nowak, M. J.; Lapinski, L.; Bieńko, D. C.; Michalska, D. Spectrochim Acta 1997, A35, 855.
41. Milburn, G. H. W.; Truter, M. R. J Chem Soc A 1966, 1609.
42. Shandles, R.; Schlemper, E. O.; Murmann, R. K. Inorg Chem 1971, 10, 2785.
43. Atoji, M.; Richardson, J. W.; Rundle, R. E. J Am Chem Soc 1957, 79, 3017.
44. Nakamoto, K.; McCarthy, P. J.; Fujita, J.; Condrate, R. A.; Behnke, G. T. Inorg Chem 1965, 4, 36.
45. Hiraishi, J.; Nakagawa, I.; Shimanouchi, T. Spectrochim Acta 1968, 24A, 819.
46. Raudaschl, G.; Lippert, B.; Hoeschele, J. D.; Howard-Lock, H. E.; Lock, C. J. L.; Pilon, P. Inorg Chim Acta 1985, 106, 14.
47. Degen, I. A.; Rowlands, A. J. Spectrochim Acta 1991, 47A, 1263.
48. Nakamoto, K. Infrared and Raman Spectra of Inorganic and Coordination Compounds; Wiley: New York, 1997, part B, Chap. III.
49. Barańska, H.; Kuduk-Jaworska, J.; Cacciari, S. J Raman Spectrosc 1997, 28, 1.
50. Wysokiński, R.; Michalska, D. to be published.
51. Beagley, B.; Cruickshank, D. W. J.; McAuliffe, C. A.; Pritchard, R. G.; Zaki, A. M.; Beddoes, R. L.; Cernik, R. J.; Mills, O. S. J Mol Struct 1985, 130, 97.
52. Soltzberg, L.; Margulis, T. M. J Chem Phys 1971, 55, 4907.
53. Tornaghi, E.; Andreoni, W.; Carloni, P.; Hutter, J.; Parrinello, M. Chem Phys Lett 1995, 246, 469.